BOLETIN DE LA SOCIEDAD ESPAÑOLA DE
Cerámica y Vidrio
A R T I C U L O

Consolidation of flaw-tolerant layered structures by the insertion of reactive layers

B. FERRARI [1], S. BUENO[1,2] C. BAUDÍN[1]

[1]Instituto de Cerámica y Vidrio, CSIC, E-28049, Madrid, SPAIN
[2] Fundación Innovarcilla - Centro Tecnológico de la Cerámica de Andalucía. Pol. Ind. El Cruce. Los Alamillos, 25. 23710 Bailén, Spain

The processing parameters to obtain a laminate consisting of very thin alumina-aluminium titanate crack deflecting layered structures sandwiched between relatively thick load bearing alumina layers are described. The optimum processing conditions for the insertion of *reactive layers* to improve joining during sintering have been established. Pre-sintered alumina tapes were used as the load bearing components while the internal structures were shaped by a combination of electrophoretic deposition (EPD) and dipping. The dipped layers acted as *reactive layers* during sintering. The thickness of the dipped layers has to be controlled in order to avoid the disappearance of the EPD structure during sintering as well as the cracking of the coating during drying or handling. The specimens were mechanically tested in three points bending with the applied load perpendicular to the layers and the fracture surfaces were observed by scanning electron microscopy. The obtained structure presents crack deflection at the microstructural scale during fracture which confers it flaw tolerance.

Keywords: Alumina, Aluminium Titanate, Multilayers, flaw defleccion

Consolidación de estructuras laminadas tolerantes a los defectos mediante capas reactivas

Se describen los parámetros de procesamiento mas adecuados para obtener laminados constituidos por capas finas de alúmina-titanato de aluminio deflectoras de grietas alternadas con capas gruesas de alúmina resistentes a las cargas. Estas últimas se han fabricado a partir de láminas obtenidas por colaje en cinta y presintetizadas. Las estructuras con capacidad para la deflexión de las grietas se conformaron mediante una combinación de deposición electroforética e inmersión. Se han establecido las condiciones óptimas para que las capas obtenidas por inmersión actúen como capas reactivas durante la sinterización, sin que desaparezca la estructura EPD durante la sinterización ni se produzca el agrietamiento durante el secado y la manipulación de la estructura. El comportamiento mecánico de las estructuras laminadas obtenidas se analizó mediante ensayos de flexión en tres puntos, con la carga aplicada en la dirección perpendicular a la superficie de las capas, y observaciones fractográficas. La estructura óptima obtenida es tolerante a las grietas debido a la deflexión de éstas por las capas internas durante la fractura.

Palabras clave: Alúmina, Titanato de aluminio, Multicapas, deflexión de grieta

1. INTRODUCTION

Ceramic laminates are being developed to overcome the lack of mechanical reliability of ceramics[1,2]. Since the seminal work by Clegg et al.[3], a number of ceramic-ceramic layered composites with weak interfaces between layers to originate crack deflection have been proposed. In this sense, laminates constituted by relatively stiff and brittle external layers, and microcracked internal layers to produce multiple crack deflection at the microstructural scale, have been processed and characterised[4]. The main hypothesis of this approach is that the limitation of delamination lengths avoids the loss of structural integrity. Structures containing very thin layers should be envisaged to extend this laminate concept to coatings.

The potential of the alumina (Al_2O_3)-titania (TiO_2) system to fabricate laminates with very thin oxide deflecting layers was explored in a previous work[5]. Sandwich structures formed by two external alumina tapes and one internal alumina/titania layered structure were developed. Two different internal layered structures were studied in order to analyse the effect of the thickness of the constituent layers on the fracture behaviour. The layers with the largest amounts of titania presented high porosity and extensive delamination occurred through them for both studied structures whereas the alumina-rich layers acted as ligaments. The thickness of the alumina-rich layers determined the fracture mode: the presence of relatively thin layers led to structures with higher capacity for strain whereas thicker layers led to higher ultimate failure loads.

In this work the design of the laminate was changed to improve its mechanical response by limiting the delamination lengths and increasing the proportion of load bearing constituents. First, three tapes were used as load bearing constituents instead of two which placed the internal layered structures far from the maximum shear stress when subjected

to bending. Second, the proportion of titania in the composite layers was lowered in order to decrease porosity in the titania-rich layers.

The processing route was the pilling up of pure alumina cast tapes coated by layered structures shaped by electrophoretic deposition (EPD), as explained elsewhere[5]. In order to improve the joining between the pre-sintered tapes and the EPD layered structures, thin layers of pure alumina were shaped by dipping on the surfaces of the pre-sintered tapes. Such layers made of reactive powder are much more active during sintering than the pre-sintered ones. In fact, thin coatings of pure zirconia (m-ZrO_2[6] and t-ZrO_2[7]) and nickel[8] obtained by dipping have successfully been used to join green tapes of Al_2O_3/Y-TZP and dense metallic Ni plates to Al_2O_3/Ni layers, respectively. In those laminates, the components (Al_2O_3 and ZrO_2) or the sintering conditions (Al_2O_3 and Ni) prevented the reaction between layers. It was our hypothesis that the reaction during sintering of the non-compatible compounds Al_2O_3 and TiO_2 [9] should contribute to the joining process during the thermal treatment in the proposed laminate.

In this work, the effect of the shaping parameters of the *reactive layers* on the microstructure and the structural integrity of the laminate are studied and the optimum shaping conditions are presented.

2. EXPERIMENTAL

Powders of alumina (α-Al_2O_3, Condea HPA05, USA) and titania (TiO_2 – anatase, Merck808, Germany) were used as starting materials. Al_2O_3 powders have a mean particle size of 0.4 μm and a specific surface area of 10 m^2/g, while TiO_2 powder have a mean particle size of 0.3 μm and a surface area of 9 m^2/g. Stabilization of suspensions of both powders in ethanol has been reported elsewhere[5].

For the shaping processes, stabilized suspensions of pure alumina (A) and 50/50 vol.% Al_2O_3/TiO_5 (AAT) were prepared in ethanol to a final solid contents of 3 vol.%, adding polyethylene imine (PEI, Aldrich, Germany) and sonicating for 2 min. Additional pure alumina suspensions with 10 and 15 vol.% of solid contents were prepared. Alumina substrates (≈12 mm x 35 mm surface and 400 μm thickness) were prepared by cutting cast tapes pre-sintered at 900ºC for 1h to reach ≈ 20-25 vol.% of open porosity.[5]

Two kinds of coated pre-sintered alumina tapes were prepared, as shown in figure 1. The two-side *monolayer coated* tapes (Fig. 1 a) were shaped by dipping the pre-sintered tapes in a suspension made of pure alumina. The one-side *multilayer coated* tapes (Fig. 1 b) were obtained by sequential EPD of AAT and A suspensions on one of the sides of the *monolayer coated* tapes. The other side was masked with graphite during the EPD process.

The EPD experimental setup and the sequential EPD performance was described elsewhere[5]. A power source (AMEL mod. 551, Great Britain) was used for EPD. Films of different compositions were built under galvanostatic conditions, maintaining electric fields ranging from 4 to 5 V/cm in the electrophoretic cell. The deposition time was 3 min in all cases.

Coating by dipping was done with pure alumina suspensions with three different solid loadings (3, 10 and 15 vol.%). The alumina substrates were dipped to assure the saturation of the porous structure. Substrates withdrawal was performed with a lift at a constant rate of 7.5 mm/s. To increase the thickness of the films, dipping was repeated up to 3 times drying the tape between two sequential dip-processes. The amount of material deposited by EPD and dipping was quantified in terms of mass per unit coated area after drying.

The final symmetric layered structures to be sintered (Fig. 2) were obtained by sandwiching one *monolayer coated* alumina tape (Fig 1 a) between two one-side *multilayer coated* tapes with both multilayer coatings in contact with the central tape (Fig. 1b).

A two step sintering schedule (1200ºC-4h and 1450ºC-2h, heating and cooling rates 2ºC/min) was used. In order to enhance the joining, a small load (≈115 g) was placed on top of the structures.

TABLE I: MASS GAIN VALUES FOR THE DIFFERENT DIPPING CONDITIONS USED (ANALYTICAL BALANCE ERROR ± 0.2).

		Solid Concentration		
Number of dips		**3 vol.%**	**10 vol.%**	**15 vol.%**
	1	2.0 mg/cm²	2.4 mg/cm²	5.5 mg/cm²
	2	2.8 mg/cm²	3.2 mg/cm²	10.6 mg/cm²
	3	4.7 mg/cm²	Cracking during drying	Cracking during drying

Figure 1: Scheme of the green coated structures used to fabricate the laminates.

(a) Two-side *monolayer coated* structure shaped by dipping a pre-sintered alumina tape. From the bottom to the top of the structure: $A_{dip}/A_{tape}/A_{dip}$.

(b) One-side *multilayer coated* structure shaped by EPD on one of the faces of a two-side *monolayer coated* structures (a). From the bottom to the top of the structure: $A_{dip}/A_{tape}/A_{dip}/AAT_{EPD}/A_{EPD}/AAT_{EPD}$.

A_{dip}: thin alumina layer obtained by dipping A_{tape}: pre-sintered alumina tape. AAT_{EPD}: multilayer structure shaped by EPD of the alumina (A) and composite (AAT) suspensions.

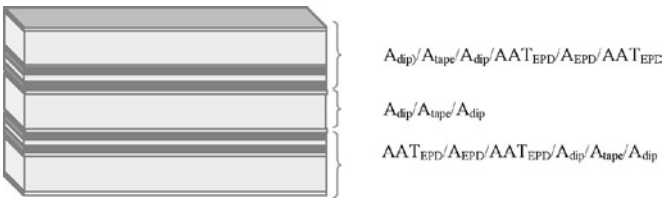

Figure 2: Scheme of the final symmetric layered structure to be sintered. Nomenclature is the same as in figure 1.

Five "as sintered" specimens (≈35 mm x 12 mm x 1.2 mm thick) of each structure were tested in three point bending (Fig. 2) using stainless steel supports and an universal testing machine (20 mm span, 0.5 mm·min^{-1}; Microtest, Spain) and the fracture surfaces were analysed by Scanning Electron Microscopy (SEM, Zeiss DSM-400, Germany).

3. RESULTS AND DISCUSSION

Table I summarises the mass gains of the alumina substrates tapes after drying for the three different dip coating conditions used. An upper limit for the deposited mass to avoid the cracking of the films during drying is apparent. From these results, three structures with the tapes prepared by dipping twice, leading to coatings of 2.8, 3.2 and 10.6 mg/cm^2 for 3, 10 and 15 vol.% suspensions, were fabricated. Additionally, an uncoated alumina tape was taken as reference. The EPD of the multilayered coatings (AAT/A/AAT) on dipped and non-dipped Alumina tapes, led to substrate mass gains of around 43-47 mg/cm^2.

Sintered structures processed using non-dipped alumina tapes and a tapes dipped in the 15 vol.% alumina suspension exhibited incomplete structure joining and failure of the specimens occurred during handling. Conversely, those specimens processed from structures obtained by dipping into the 3 and 10 vol.% suspensions were successfully sintered. Results demonstrate that effective reaction sintering occurs only when both layers in contact are made of reactive powders, such as the dipped *reactive alumina layer* and the EPD ones, and not when one of the structures in contact has just been pre-sintered. Hence, pre-sintered tapes have to be coated by *reactive layers* to provide the structure joining during sintering.

It is also clear that there is an upper limit for the thickness of the dipped layers to avoid specimen failure. This limit should come from the fact that, even tough the concentrations of the suspensions used for dipping in this work are suitable to obtain thin and low packing density reactive layers, they are much lower than those optimum for the dipping process[6-8]. The thick layers with low packing density obtained for the 15 vol.% suspension lacked structural integrity and originated the failure of the structure during handling, limiting the thickness of the dipped *reactive layers* allowed.

On the basis of the above discussed results, specimens fabricated following the two processing routes that led to laminates with structural integrity were used for mechanical testing. Thus, two series of specimens were fabricated using tapes dipped twice in the suspensions containing 3 and 10 vol.% of solids; they will be named S3 and S10, respectively.

In figure 3, the load-displacement curves for different specimens were fairly coincident. The S3 specimens failed catastrophically and at higher loads than the S10 specimens. The load-displacement curves for these latter presented three distinct load drops at load levels significantly lower than those corresponding to the S3 specimens. No delamination was observed in the S3 specimens whose fracture surfaces showed no differentiated layers, whereas extensive delamination was observed in the case of S10 specimens. This shows that there is a lower limit for the thickness of the joining *reactive layer* that allows the complete inter-diffusion between the EPD structures with the dipped films and the cast tapes leading to

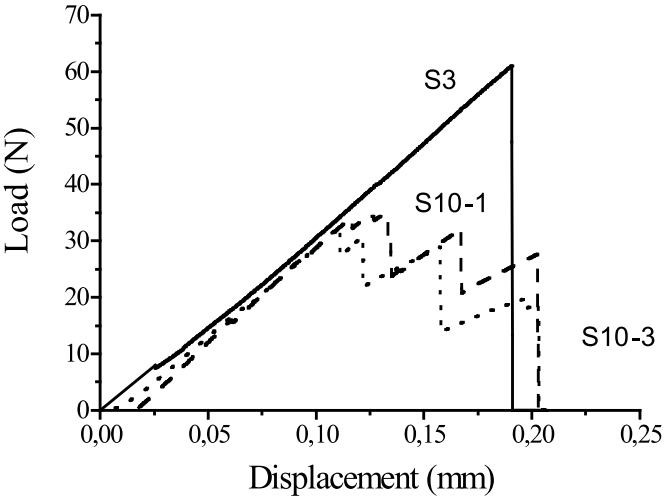

Figure 3: Characteristic load-displacement curves. S3: specimen showing brittle fracture. S10-1 and S10-3: two nominally identical S10 layered specimens. Three peak loads followed by a slope decrease are observed. Calculated engineering strengths at the peak loads are 60, 125 and 437 MPa for S10-1 and 72, 145 and 408 MPa for S10-3.

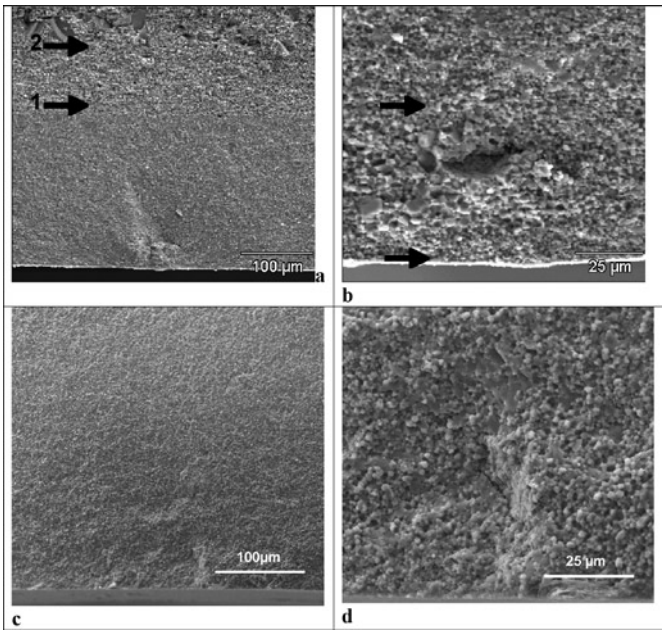

Figure 4: Characteristic features found in the fracture surfaces of the studied laminates. The lower parts of the micrographs correspond to the tensile surfaces of the specimens. SEM micrographs.

a) Specimen S10, first alumina tape. Fracture from a critical defect is observed. The zones with the different fracture modes described in figure 5c are observed and indicated by arrows.

b) Specimen S10, detail of a critical defect in the first alumina tape: a pore formed by differential sintering and surrounded by large (4-8μm) alumina grains. The arrows show the limits of a zone (≈50μm width) that presents intergranular fracture.

c) Specimen S3, first alumina tape. Neither a clear fracture origin nor differentiated fracture zones are observed at this low magnification.

d) Specimen S3, a thin laminar pore is observed in the zone close to the surface in tension. The surrounding microstructure presents the same aspect as the rest of the tape.

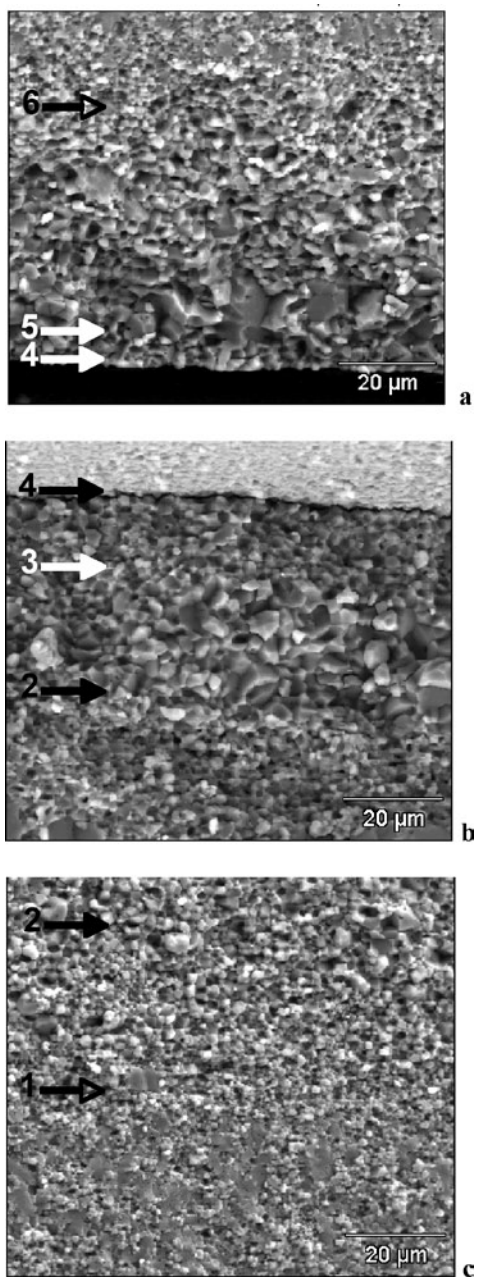

Figure 5: Characteristic features of the fracture surfaces of the studied materials. SEM micrographs. The direction of crack propagation was from bottom to top of the micrographs.

a) Arrow 4 as in figure 5b. Arrow 5: Interface between the second biphasic layer and the second large grained alumina layer. Alumina grain size decreases progressively towards the bulk of the tape. Arrow 6: The original microstructure of the central alumina tape is observed at the top of the micrograph.

b) Arrow 2 as in figure 5c. Arrow 3: Interface between the large grained alumina and the second biphasic layer. Arrow 4: Delamination across the second biphasic layer.

c) The bulk of the first alumina tape is shown at the bottom of the micrograph. Zones signalled with arrows 1 and 2 correspond to those in figure 4a. Arrow 1: Interface between the first alumina tape and the first biphasic layer with small grain size. The changing from the characteristic transgranular fracture of the bulk of the tape into intergranular fracture is observed. Arrow 2: Interface between the first biphasic layer and the first alumina layer with large grain size; mostly intergranular fracture is observed.

the disappearance of the layered structure during sintering, and the associated brittle failure mode.

In general, composite beams fail by the combination of shear and tensile stresses, the shear stresses being the maximum at the neutral fibre of the beam[10]. The ratio between the maximum shear, $\tau_{max,}$ and tensile, σ_{max}, stresses is given by:

$$\tau_{max} / \sigma_{max} = h / 2 L \quad (1)$$

where, h and L are the height of the specimen and the span of the testing device, respectively. Shear fracture would lead to the decrease of the specimen compliance and, consequently, the strength of the specimens. For the geometry of the specimens used here, the relationship of eq. (1) is 0.05. Taking into account the values of the maximum loads sustained by the S10 specimens that corresponded to the first load drops in the load-displacement curves (Fig. 3), upper limits for the maximum tensile stresses of 61±9 MPa are calculated. Thus, maximum shear stresses of about 3 MPa were expected during testing. This value is much lower than reported values for the shear strength of alumina (≈ 110 GPa[11]) which constituted the central layer, where the neutral fibre of the specimens was located. Therefore, failure of the specimens would be initiated by tensile stresses at the surface of the external alumina tape placed in tension during testing.

In all S10 specimens, fracture was initiated at pores of irregular shapes and surrounded by large alumina grains (Fig. 4a-b) whereas no clear failure origins could be detected in the S3 specimens (Fig. 4c) where relatively small defects were observed close to the surfaces in tension during the bending test (Fig. 4d). In this latter case, the aspect of the microstructure and failure mode of alumina was the same through the whole alumina tapes. On the contrary, significant growth of the alumina grains (up to 8μm) occurred in the region of fracture initiation in the S10 specimens and fracture was mostly intergranular in a region up to ≈50μm depth from the tensile surface (Fig. 4b) while far from the surface (Fig. 4a) the tapes presented their characteristic transgranularafracture[5].

The differentiated regions observed in the S10 specimens that were not observed in the specimens processed from the lowest concentrated slip (S3), have to be formed by the reactive alumina deposited and/or infiltrated during the dipping process. The large alumina grains presenting intergranular fracture in alumina-aluminium titanate based laminates are characteristic of the evolution of alumina particles in the presence of titania traces during sintering[5]. Most probably small amounts of titania reached the masked surfaces of the tapes during the EPD process. Nevertheless, results indicate that a sufficient amount of reactive alumina such as that in the S10 specimens has to be present for the titania to have a significant effect on the microstructural evolution of the tape. In fact, the large alumina grains developed at the S10 laminates were neither visible in the S3 specimens nor in the un-dipped samples studied previously[5]. Therefore, in further laminate design dipped coatings of the external surfaces should be eliminated.

Figures 5 to 7 show different details of the fracture of the S10 laminates. Interfaces between layers with different microstructures can be observed. The following discussion on the micrographs is done from the bulk of the first tape that had its surface in tension during testing (Figure 5c) to the upper surface of the specimens in compression during testing

(Figure 7a). Thus, the micrographs in figure 5 and 7 will be described in reverse order (from 5c to 5a in figure 5 and from 7b to 7a in figure 7). Characteristic features of the initiation of the fracture from the surface in tension of the first tape for the S10 specimens above discussed are shown in figure 4 a-b.

In the bulk of the first alumina tape, far (≈50μm) from the tensile zone of the specimens, fracture was mostly transgranular to reach a differentiated layer of 35-40μm thickness with smaller grain size and where significant amounts of Ti were detected by EDX (Figs. 4a, 5c, between arrows 1-2). This composite layer presented the typical intergranular fracture of alumina/aluminium titanate composites fabricated by reaction sintering[5]. As no differentiated pure alumina layer that could correspond to the original dipped one was found, the observed composite layer should correspond to the combined evolution of the dipped alumina and the EPD composite layers during sintering. The biphasic layer finished at a large grained alumina layer 20-25μm thick (Fig. 5b from arrow 2 and Fig 5c between arrows 2-3) in which Ti traces were detected by EDX, with the characteristic intergranular fracture observed in TiO_2-doped alumina[5]. This layer has to be identified with the evolution of the EPD alumina layer during sintering. TiO_2 will diffuse into it leading to the grain growth observed, as occurred in other alumina/aluminium titanate laminates. After the alumina layer a biphasic one corresponding to the second EPD composite layer was observed, (Fig. 5b arrow 3). The crack was deflected inside this layer as shown in figures 5b and 5a (arrow 4) in which different parts of the composite layer are observed at different levels of the fracture surface. This layer ended again in a large grained alumina layer, with intergranular fracture (Fig. 5a, arrow 5) in which grain size decreased progressively, as the distance to the interface with the biphasic layer increased up to the point where the microstructure of the original tape with mostly transgranular fracture was recovered (Fig. 5a, arrow 6). The alumina layer starting in arrow 5 (Fig. 5 a) should be originated from the original dipped coating of the central tape which indicates the dramatic differences between the alumina microstructure depending on the shaping process. When the composite layers were shaped by EPD on the dipped alumina the interaction between them and the reactive layer led to the formation of a single composite layer (Fig. 5c between arrows 1-2). On the contrary, the evolution of the dipped and EPD layers was mostly independent when they were shaped independently (Fig. 5b and 5a).

It was not possible to discern defects as fracture origins of the central alumina tapes (Fig. 6a) and the second surface tapes (Fig. 6b) in any of the tested specimens. In those zones,

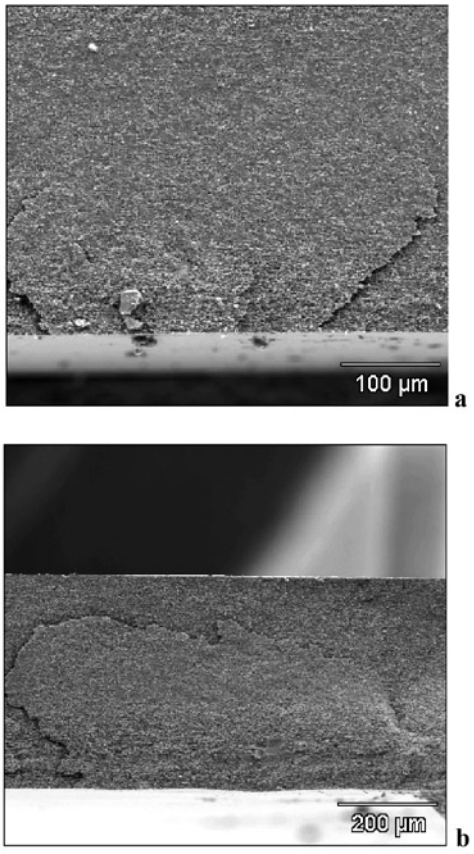

Figure 6: Characteristic features of the fracture surfaces of the studied materials. SEM micrographs. Initiation of the fracture at the central (a) and second external (b) tapes. No singular critical defects are present. Multiple planes of crack propagation perpendicular to the applied stress are observed.

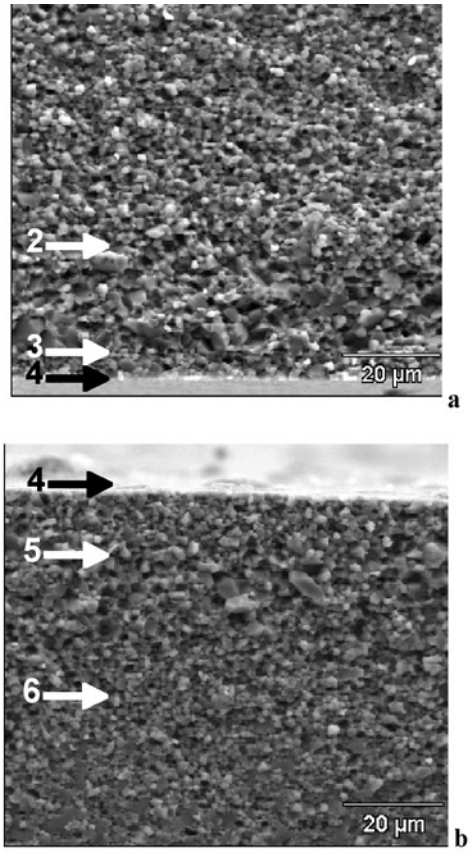

Figure 7: Characteristic features of the fracture surfaces of the studied materials. SEM micrographs. The direction of crack propagation was from bottom to top of the micrograph.
a) The second external alumina tape is located at the top of the micrograph. The same features as is figure 5b are observed.
b) Fracture of the top part of the central alumina tape. It presents the same features as the bottom part of the tape (Fig. 5a). Numbered arrows signal to the observed features.

fracture occurred across different planes perpendicular to the applied stress.

As shown in figure 7b, the characteristic features observed at the other end of the central alumina tape were similar to those just described. The grain size as well as the proportion of intergranular fracture increased progressively to reach a large grain sized alumina layer which ended in a biphasic layer through which the crack was deflected. The central tape was originally dipped in alumina and sandwiched between two composite layers for sintering. Thus, the microstructural development was symmetrical as shown in figures 5a and 7b.

The microstructural symmetry observed in the central tape was also found for the two external tapes. As shown in figures 5b and 7a, the same features were found at the bottom part of the second external alumina tape and in the top part of the first one. Both structures were in contact with the central tape and with EPD layers following the sequence AAT/A/AAT in figure 2. After the biphasic layer through which the crack was deflected (Fig. 7a-b) a large grained monophase alumina layer followed by another biphasic layer (Fig. 7b) and farther, the characteristic fracture of the original tape were found. Numbered arrows point out the interfaces between layers similar to those noted in figure 5.

The crack deflection through the biphasic layers (Figs. 5a-b and 7, arrow 4) demonstrates the high quality of the joining between the EPD structures and the dipped central alumina tapes developed during sintering. Once the main crack was deflected, fracture started again by the cooperative effect of different parallel cracks traversing the central alumina tapes (Fig. 6a). The same process occurred at the layered structure between the central tape and the second external one (Fig. 6b and 7).

All load-displacement curves for the S10 specimens showed three distinct load peaks with subsequent slope decreases. The three alumina tapes were the load bearing elements in the laminates. Consequently, their fracture would originate load drops, while the deflection of the cracks across the layered composite structures would lead to load increases. As the fracture of one tape would involve a significant increases of the specimen flexibility, the load increase after the fracture of a tape will take place with lower slope. Thus, each load drop observed in the load-displacement curves of the S10 specimens can be identified with the fracture of the alumina tape (in the case of the first tape) plus the part of the EPD layered structure (in the case of the second and third tapes).

Failure strengths for the S10 specimens at each load drop can be calculated assuming that each one corresponds to the fracture of one alumina tape and not considering the width of the EPD layers. The strengths corresponding to the first partial fractures of the specimens (61±9 MPa) were low due to the large critical defects observed (Fig. 4a-b). The second and third load drops, corresponding to the fracture of the central and second surface tapes occurred at increasing strengths (121±19 and 445±52 MPa respectively). Moreover, the relative variability of strength values for the final failure of the specimens (≈7%) was much lower than that of the two previous partial fractures (≈13-15%).

CONCLUSIONS

A layered structure with very thin layers that deflect cracks at the microstructural scale has been developed in the system alumina-titania. The pilling up of alumina cast tapes coated with composite layered structures shaped by dipping and EPD have been established as adequate processing method for this kind of materials.

Reactive layers should be intercalated between the alumina cast tapes and those coated by EPD to promote joining during sintering. Dip-coating at low solid contents has been demonstrated to be an adequate process to fabricate the reactive layers which optimization determines the characteristic of the joining and hence the associated fracture response of the layered composite.

Further studies should be done in order to avoid the dip-coating of the external surfaces of the specimens to increase their initial strength.

ACKNOWLEDGEMENTS

The authors gratefully acknowledge financial support from the Spanish Science and Education Ministry (MEC) through Projects MAT2006-13480 C02-01 and MAT2006-01038 (Spain).

REFERENCES

1. M. Anglada, E. Jiménez-Piqué and P. Hvizdos, in: "Layered, Functional Gradient Ceramics, and Thermal Barrier Coatings: Design, Fabrication and Applications", Trans. Tech. Publications Ltd., Stafa-Zuerich, Switzerland, 2007.
2. W. J. Clegg, "Design of ceramics laminates for structural applications", Mater. Sci. Technol., 14, 483-95 (1998).
3. W. J. Clegg, K. Kendall, N. McAlford, J. D. Birchall and T. W. Button, "A simple way to make tough ceramics", Nature, 347, 45-47 (1990).
4. S. Bueno and C. Baudín, "Design and processing of a ceramic laminate with high toughness and strong interfaces", Composites Part A, 40, 137-143 (2009).
5. B. Ferrari, A. Bartret and C. Baudín, "Sandwich materials formed by thick alumina tapes and thin-layered alumina-aluminium titanate structures shaped by EPD", J. Eur. Ceram. Soc., 29, 1083-90 (2009).
6. I. Nikolaidis, J. Gurauskis, C. Baudin, R. Moreno and A. J. Sanchez-Herencia, "Forming of ceramic laminates comprising thin layers of a few particles", J. Am. Ceram. Soc., 91, 2124-2129 (2008).
7. M. G. Pontin, F. F. Lange, A. J. Sanchez-Herencia and R. Moreno, "Effect of unfired tape porosity on surface film formation by dip coating", J. Am. Ceram. Soc., 88, 2945-2948 (2005).
8. B. Ferrari, A. J. Sanchez-Herencia and R. Moreno, "Nickel-alumina graded coatings obtained by dipping and EPD on nickel susbtrates", J. Eur. Ceram. Soc., 26, 2205-22012 (2006).
9. R. Uribe, C. Baudín, "Formación de titanato de aluminio por reacción en estado sólido de alúmina y titania", Bol. Soc. Esp. Ceram. Vidr., 39 (2) 1-10 (2000).
10. J. V. Mullin and A. C. Knoell, "Basic concepts in composite beam testing", Mater. Res. Standards, 10, 16-20 (1970).
11. X. Wang and N. P. Padture, "Shear strength of ceramics", J. Mater. Sci., 39, 1891-1893 (2004).

Recibido: 15-9-09
Aceptado: 30-10-09